Spin-dependent tunneling characteristics of fully epitaxial magnetic tunneling junctions with a full-Heusler alloy Co_2MnSi thin film and a MgO tunnel barrier

T. Ishikawa, T. Marukame, H. Kijima, K.-I. Matsuda, T. Uemura, M. Arita, and M. Yamamoto[a)]

Division of Electronics for Informatics, Graduate School of Information Science and Technology, Hokkaido University, N14, W9, Kita-ku, Sapporo 060-0814, Japan

(Received 31 August 2006; accepted 18 September 2006; published online 7 November 2006)

Fully epitaxial, exchange-biased magnetic tunnel junctions (MTJs) were fabricated with a Co-based full-Heusler alloy Co_2MnSi (CMS) thin film as a lower electrode, a MgO tunnel barrier, and a $Co_{50}Fe_{50}$ upper electrode. The microfabricated CMS/MgO/$Co_{50}Fe_{50}$ MTJs exhibited relatively high tunnel magnetoresistance ratios of 90% at room temperature and 192% at 4.2 K. The bias voltage dependence of differential conductance (dI/dV) for the parallel and antiparallel magnetization configurations suggested the existence of a basic energy gap structure for the minority-spin band of the CMS electrode with an energy difference of about 0.4 eV between the bottom of the vacant minority-spin conduction band and the Fermi level. © *2006 American Institute of Physics*. [DOI: 10.1063/1.2378397]

Employing spin-polarized electrons is essential for spintronic devices. Due to the existence of an energy gap at the Fermi level (E_F) for one spin direction, half-metallic ferromagnets are characterized by a complete spin polarization at E_F,[1] so these are the most promising ferromagnetic electrode materials for spintronic devices. Co-based full-Heusler alloys have been extensively studied recently as candidates for use in half-metallic ferromagnetic electrodes[2,3] and regarding their application to magnetic tunnel junctions (MTJs).[4–13] This is because of the half-metallic ferromagnetic nature theoretically predicted for some of these alloys[14,15] and because of their high Curie temperatures, which are well above room temperature (RT).[16] One Co-based full-Heusler alloy, in particular, Co_2MnSi (CMS), has attracted interest because of its half-metallic nature theoretically predicted, with a large energy gap of 0.42 eV (Ref. 14) to 0.81 eV (Ref. 15) for its minority-spin band, and its high Curie temperature of 985 K.[16] Sakuraba *et al.* reported a high tunneling magnetoresistance (TMR) ratio of 570% at 2 K (67% at RT) for MTJs consisting of an epitaxial CMS lower electrode, an amorphous AlO_x tunnel barrier, and a highly oriented CMS upper electrode.[11] We recently developed fully epitaxial MTJs with a Co-based full-Heusler alloy (Co_2YZ) thin film of either $Co_2Cr_{0.6}Fe_{0.4}Al$ (CCFA) (Refs. 7–9) or Co_2MnGe (Refs. 8 and 10) as a lower electrode and a MgO tunnel barrier and have demonstrated a relatively high TMR ratio of 90% at RT (240% at 4.2 K) for fully epitaxial CCFA/MgO/$Co_{50}Fe_{50}$ MTJs.[9]

We have developed fully epitaxial MTJs with a CMS thin film as a lower electrode and a MgO tunnel barrier in the present study and have investigated their spin-dependent tunneling characteristics.

We will now describe the fabrication of fully epitaxial MTJs with a CMS thin film and a MgO tunnel barrier. To realize exchange biasing in these fully epitaxial MTJs, we used an upper electrode of $Co_{50}Fe_{50}$ in a $Co_{50}Fe_{50}$ (3 nm)/Ru interlayer (0.8 nm)/$Co_{90}Fe_{10}$ (2 nm) trilayer, which was exchange biased with an IrMn antiferromagnetic layer through the $Co_{90}Fe_{10}$/IrMn interface. The fabricated MTJ layer structure was as follows: MgO buffer layer (10 nm)/CMS lower electrode (50 nm)/MgO tunnel barrier (2.4 nm)/$Co_{50}Fe_{50}$ upper electrode (3.5 nm)/Ru interlayer (0.8 nm)/$Co_{90}Fe_{10}$ (2 nm)/$Ir_{21.5}Mn_{78.5}$ (IrMn) (10 nm)/Ru cap (5 nm), grown on a MgO (001) single-crystal substrate. Each layer in the MTJ structure was successively deposited in an ultrahigh vacuum chamber (with a base pressure of $\sim 8\times10^{-8}$ Pa) through the combined use of magnetron sputtering and electron beam (EB) evaporation.

The CMS layer was deposited on a MgO buffer layer by magnetron sputtering at RT and subsequently annealed *in situ* at 600 °C for 15 min. The thus obtained 50-nm-thick CMS films had sufficiently flat surface morphologies with rms roughness of about 0.22 nm. Through x-ray pole figure measurements, we confirmed that the CMS films annealed at 600 °C grew epitaxially and crystallized into the ordered $L2_1$ structure.[17] We determined that the CMS film composition was $Co_{2.0}Mn_{0.84}Si_{0.80}$ through inductively coupled plasma analysis.

The MgO tunnel barrier was deposited by EB evaporation at RT. The layers of $Co_{50}Fe_{50}$, Ru, $Co_{90}Fe_{10}$, and IrMn were all deposited by magnetron sputtering at RT. Reflection high-energy electron diffraction (RHEED) patterns observed *in situ* for each layer during fabrication clearly indicated that all the layers of the CMS lower electrode, MgO tunnel barrier, $Co_{50}Fe_{50}$ upper electrode, Ru ultrathin interlayer, $Co_{90}Fe_{10}$ layer, and IrMn layer grew epitaxially. We fabricated fully epitaxial MTJs with the layer structure described above by using photolithography and Ar ion milling. The fabricated junction size was 10×10 μm^2. As shown below, as-fabricated (i.e., not *ex situ* annealed) MTJs showed clear exchange-biased TMR characteristics. The MTJs of which transport properties will be described below are as-fabricated MTJs.

Figure 1 shows a cross-sectional high-resolution transmission electron microscope lattice image of a fabricated

a)Author to whom correspondence should be addressed: electronic mail: yamamoto@nano.ist.hokudai.ac.jp

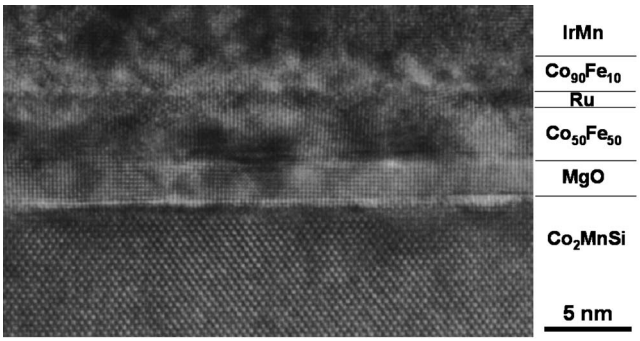

FIG. 1. Cross-sectional high-resolution transmission electron microscopy lattice image of a MTJ layer structure consisting of CMS (50 nm)/MgO barrier (2.4 nm)/$Co_{50}Fe_{50}$ (3.5 nm)/Ru interlayer (0.8 nm)/$Co_{90}Fe_{10}$ (2 nm)/IrMn (10 nm) along the [110] direction of the CMS.

MTJ layer structure. This image clearly shows that all the layers from the CMS lower electrode to the IrMn layer were grown epitaxially and were single crystalline, although the detailed structures of the successive layers from the Ru interlayer to the IrMn layer were not fully analyzed. Figure 1 also shows that extremely smooth and abrupt interfaces were formed in the CMS/MgO/$Co_{50}Fe_{50}$ trilayer.

Figure 2(a) shows typical magnetoresistance curves at a bias voltage (V) of 5 mV at RT and 4.2 K for an as-fabricated CMS/MgO/$Co_{50}Fe_{50}$ MTJ. Clear exchange-biased TMR characteristics were obtained with relatively high TMR ratios of 90% at RT and 192% at 4.2 K. Figure 2(b) shows the TMR ratio at V=5 mV, as well as RA_{AP} and RA_P as a function of temperature (T) from 4.2 to 297 K, where RA_{AP} and RA_P are the respective resistance-area products for the antiparallel and parallel magnetization configurations between the upper and lower electrodes. As T decreased from RT to 4.2 K, the TMR ratio increased by a factor of 2.1. If we use parameter $\gamma=\alpha(4.2\ \mathrm{K})/\alpha(\mathrm{RT})$, where α is the TMR ratio, to represent the degree of temperature dependence of the TMR ratio, γ for the fabricated CMS/MgO/$Co_{50}Fe_{50}$ MTJs was 2.1. This value of γ was much lower than the value γ=8.1 previously reported for CMS/AlO_x/CMS-MTJs (a TMR ratio of 570% at 2 K and 67% at RT).[11] As shown in Fig. 2(b), RA_{AP} also increased with decreasing T, while RA_P was almost independent of T. These behaviors were similar to that previously reported for $Co_{70}Fe_{30}$/MgO/$Co_{84}Fe_{16}$ MTJs by Parkin *et al.*[18]

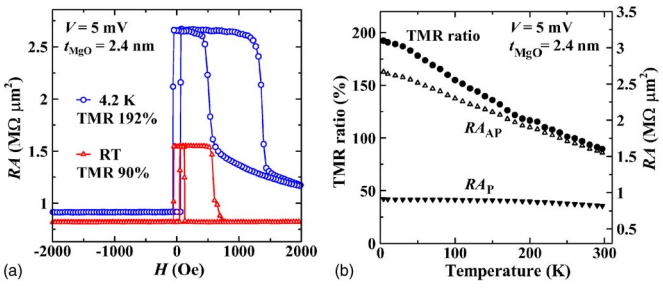

FIG. 2. (Color online) (a) Typical magnetoresistance curves at a bias voltage (V) of 5 mV at RT and 4.2 K for an as-fabricated CMS/MgO/$Co_{50}Fe_{50}$ MTJ. (b) TMR ratio at V=5 mV, as well as RA_{AP} and RA_P as a function of temperature from 4.2 to 297 K, where RA_{AP} and RA_P are the respective resistance-area products for the antiparallel and parallel magnetization configurations between the upper and lower electrodes.

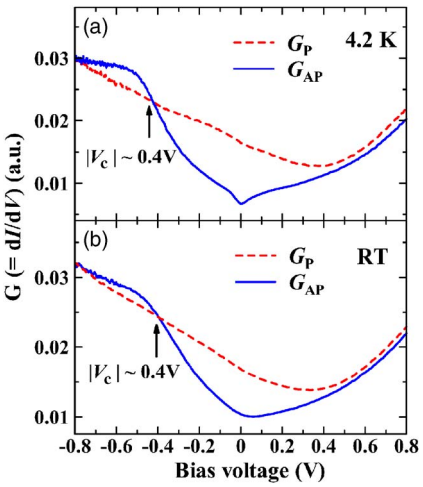

FIG. 3. (Color online) Bias voltage dependence of the differential conductances G_P and G_{AP} of an epitaxial Co_2MnSi/MgO/$Co_{50}Fe_{50}$ MTJ (a) at 4.2 K and (b) at room temperature. The bias voltage was defined with respect to the CMS lower electrode.

We deduced the spin polarization for the CMS electrodes by using Jullière's model for the TMR ratio;[19] TMR=$2P_1P_2/(1-P_1P_2)$, where P_1 and P_2 are the spin polarizations at E_F of the ferromagnetic electrodes in MTJs. As a reference sample, we fabricated fully epitaxial, exchange-biased MTJs with a layer structure of $Co_{50}Fe_{50}$ (50 nm)/MgO tunnel barrier (2.2 nm)/$Co_{50}Fe_{50}$ (3 nm)/Ru (0.8 nm)/$Co_{90}Fe_{10}$ (2 nm)/IrMn (10 nm)/Ru cap. The TMR ratios for the as-fabricated (i.e., not *ex situ* annealed) epitaxial $Co_{50}Fe_{50}$-MTJs (146% at 4.2 K and 96% at RT) indicated that the effective spin polarization (i.e., the spin polarization determined using Jullière's model for fully epitaxial, single-crystal MTJs) of the $Co_{50}Fe_{50}$ film (P_{CoFe}) was 0.65 at 4.2 K (0.57 at RT). If we estimate the effective spin polarization of the CMS film (P_{CMS}) from the TMR ratio of 192% at 4.2 K (90% at RT) for the epitaxial CMS/MgO/$Co_{50}Fe_{50}$ MTJs by using Jullière's model with P_{CoFe} of 0.65 at 4.2 K (0.57 at RT), we obtain a P_{CMS} value of 0.75 at 4.2 K (0.54 at RT). This P_{CMS} value of 0.75 at 4.2 K was much lower than the value of 1.0 theoretically predicted. Structural defects arising from deviation of the film composition from the stoichiometric one may lead to reduced spin polarization at E_F.[20,21] Thus, we can attribute the low P_{CMS} value of 0.75 at 4.2 K to the CMS film composition of $Co_{2.0}Mn_{0.84}Si_{0.80}$ significantly deviating from the 2:1:1 stoichiometric one.

We investigated the TMR ratio as a function of bias voltage V from RT to 4.2 K, where V was defined with respect to the CMS electrode. The TMR ratio exhibited a cusplike V dependence within a range of ±0.1 V around V=0 at 4.2 K, which was smeared out at RT. The bias voltages at which the TMR ratio fell to half the zero-bias value (V_{half}) were about −0.36 and +0.38 V at RT (−0.28 and +0.20 V at 4.2 K).

To further investigate spin-dependent tunneling characteristics in the CMS/MgO/$Co_{50}Fe_{50}$ MTJs, we measured the bias voltage dependence of the differential conductance ($G=dI/dV$) for the parallel and antiparallel magnetization configurations (G_P and G_{AP}, respectively) at 4.2 K and RT. Figure 3 shows $G_P(V)$ and $G_{AP}(V)$ at 4.2 K and RT. Although G_P was always greater than G_{AP} in the positive bias voltage region, a sharp increase of G_{AP} and a clear crossover between G_P and G_{AP} occurred with increasing negative bias

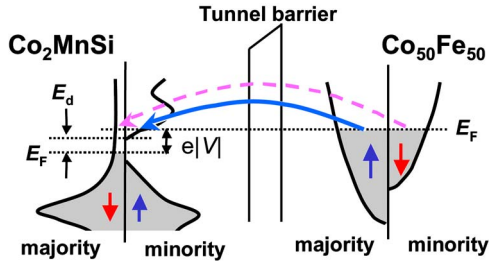

FIG. 4. (Color online) Schematic diagram of the tunneling process in a $Co_2MnSi/MgO/Co_{50}Fe_{50}$ MTJ at a negative bias voltage for the antiparallel magnetization configuration. The bias voltage was defined with respect to the CMS lower electrode. E_d represents the energy difference between the bottom of the vacant minority-spin conduction band and the Fermi level.

voltage at both 4.2 K and RT. This results in G_{AP} becoming greater than G_P in a bias voltage region beyond the characteristic voltage (V_c) of about −0.4 V at which the crossover occurs at both 4.2 K and RT. A similar crossover was also observed in the fully epitaxial $CMG/MgO/Co_{50}Fe_{50}$ MTJs for a bias voltage region with V_c of about −0.2 V (Ref. 10). In contrast, the measured $G_P(V)$ and $G_{AP}(V)$ at both RT and 4.2 K for an identically fabricated epitaxial $Co_{50}Fe_{50}/MgO/Co_{50}Fe_{50}$ MTJ showed that G_P was always greater than G_{AP} over both the positive and negative bias regions.

Taking into consideration the order of magnitude of the characteristic energy $E_c=e|V_c|$ of ~0.4 eV, the crossover can hardly be explained by inelastic tunneling via, for example, electron-magnon or electron-phonon interaction.

A possible transport mechanism leading to this notable crossover is the direct tunneling that reflects the spin-dependent density of states of the CMS electrode rather than that of the $Co_{50}Fe_{50}$ electrode. Figure 4 shows a schematic diagram explaining the spin-dependent tunneling process in the $CMS/MgO/Co_{50}Fe_{50}$ MTJs for negative V and the antiparallel configuration, where the density of states from the electronic band structure calculation for CMS by Picozzi *et al.*[15] and the density of states of the *s*-like electrons for $Co_{50}Fe_{50}$ are assumed. With this half-metallic band structure for CMS, the experimentally observed crossover can be reasonably explained as follows: the dominant tunneling process contributing to the increase of G_{AP} in the negative bias voltage region is the electron tunneling from the occupied valence band states (below E_F) in the majority-spin band of $Co_{50}Fe_{50}$ into the vacant conduction band states (above E_F) in the minority-spin band of CMS.

On the other hand, the theoretically predicted energy differences E_d between the bottom of the vacant minority-spin conduction band (above E_F) and E_F are 0.48 eV for CMS according to Picozzi *et al.*[15] and 0.055 eV according to Ishida *et al.*[14] The experimentally obtained value, ~0.4 eV, for the characteristic energy E_c of the $CMS/MgO/Co_{50}Fe_{50}$ MTJ agreed well in the order of magnitude with the E_d theoretically predicted for the minority-spin band by Picozzi *et al.*[15] Thus, the observed features in the spin-dependent G vs V characteristics in the negative bias voltage region suggest the existence of a basic energy gap structure for the minority-spin band of the CMS electrode with E_d of around 0.4 eV. This value of $E_d \sim 0.4$ eV is in contrast to a much smaller value of $E_d \sim 10-20$ meV estimated for CMS electrodes from both $CMS/AlO_x/CMS$ MTJs (Ref. 11) and $CMS/AlO_x/Co_{75}Fe_{25}$ MTJs.[13] In the above discussion, we did not explicitly consider a possible coherent tunneling process. However, even if a coherent tunneling process was involved, our interpretation is not basically altered. This is because our explanation is based on the existence of a basic energy gap structure in the minority-spin band of the CMS electrode.

In summary, we fabricated fully epitaxial, exchange-biased MTJs with a Co-based full-Heusler alloy CMS thin film as a lower electrode, a MgO tunnel barrier, and a $Co_{50}Fe_{50}$ upper electrode. Cross-sectional high-resolution transmission electron microscope observations indicated that all layers of the $CMS/MgO/Co_{50}Fe_{50}$ MTJ layer structure, including the layers for exchange biasing, were grown epitaxially and were single crystalline. The microfabricated $CMS/MgO/Co_{50}Fe_{50}$ MTJs exhibited relatively high tunnel magnetoresistance ratios of 90% at RT and 192% at 4.2 K. The bias voltage dependence of differential conductance (dI/dV) for the parallel and antiparallel magnetization configurations suggested the existence of a basic energy gap structure for the minority-spin band of the CMS electrode with an energy difference of about 0.4 eV between the bottom of the vacant minority-spin conduction band and the Fermi level.

This work was partly supported by a Grant-in-Aid for Scientific Research (B) (Grant No. 18360143) and a Grant-in Aid for Creative Scientific Research (Grant No. 14GS0301) from the Ministry of Education, Culture, Sports, Science and Technology, Japan.

[1] R. A. de Groot, F. M. Meuller, P. G. van Engen, and K. H. J. Buschow, Phys. Rev. Lett. **50**, 2024 (1985).
[2] T. Ambrose, J. J. Krebs, and G. A. Prinz, Appl. Phys. Lett. **76**, 3280 (2000).
[3] S. Wurmehl, G. H. Fecher, K. Kroth, F. Kronast, H. A. Dürr, Y. Takeda, Y. Saitoh, K. Kobayashi, H.-J. Lin, G. Schönhense, and C. Felser, J. Phys. D **39**, 803 (2006).
[4] K. Inomata, S. Okamura, R. Goto, and N. Tezuka, Jpn. J. Appl. Phys., Part 2 **42**, L419 (2003).
[5] K. Inomata, S. Okamura, A. Miyazaki, M. Kikuchi, N. Tezuka, M. Wojcik, and E. Jedryka, J. Phys. D **39**, 816 (2006).
[6] S. Kämmerer, A. Thomas, A. Hütten, and G. Reiss, Appl. Phys. Lett. **85**, 79 (2004).
[7] T. Marukame, T. Kasakara, K.-I. Matsuda, T. Uemura, and M. Yamamoto, Jpn. J. Appl. Phys., Part 2 **44**, L521 (2005).
[8] M. Yamamoto, T. Marukame, T. Ishikawa, K.-I. Matsuda, T. Uemura, and M. Arita, J. Phys. D **39**, 824 (2006).
[9] T. Marukame, T. Ishikawa, K.-I. Matsuda, T. Uemura, and M. Yamamoto, Appl. Phys. Lett. **88**, 262503 (2006).
[10] T. Marukame, T. Ishikawa, K.-I. Matsuda, T. Uemura, and M. Yamamoto, J. Appl. Phys. **99**, 08A904 (2006).
[11] Y. Sakuraba, M. Hattori, M. Oogane, Y. Ando, H. Kato, A. Sakuma, T. Miyazaki, and H. Kubota, Appl. Phys. Lett. **88**, 192508 (2006).
[12] Y. Sakuraba, J. Nakata, M. Oogane, H. Kubota, Y. Ando, A. Sakuma, and T. Miyazaki, Jpn. J. Appl. Phys., Part 2 **44**, L1100 (2005).
[13] Y. Sakuraba, T. Miyakoshi, M. Oogane, Y. Ando, A. Sakuma, T. Miyazaki, and H. Kubota, Appl. Phys. Lett. **89**, 052508 (2006).
[14] S. Ishida, S. Fujii, S. Kashiwagi, and S. Asano, J. Phys. Soc. Jpn. **64**, 2152 (1995).
[15] S. Picozzi, A. Continenza, and A. J. Freeman, Phys. Rev. B **66**, 094421 (2002).
[16] P. J. Webster, J. Phys. Chem. Solids **32**, 1221 (1971).
[17] H. Kijima, T. Ishikawa, T. Marukame, H. Koyama, K.-I. Matsuda, T. Uemura, and M. Yamamoto, IEEE Trans. Magn. **42**, 2688 (2006).
[18] S. S. P. Parkin, C. Kaiser, A. Panchula, P. M. Rice, B. Hughes, M. Samant, and S.-H. Yang, Nat. Mater. **3**, 862 (2004).
[19] M. Jullière, Phys. Lett. **54A**, 225 (1975).
[20] S. Picozzi, A. Continenza, and A. J. Freeman, Phys. Rev. B **69**, 094423 (2004).
[21] Y. Miura, K. Nagao, and M. Shirai, Phys. Rev. B **69**, 144413 (2004).